Minimizing Expected Deviation in Upper-level Outcomes Due to Lower-level Decision-making in Hierarchical Multi-objective Problems

Kalyanmoy Deb, *Fellow, IEEE*, Zhichao Lu, *Member, IEEE*, Ian Kropp, J. Sebastian Hernandez-Suarez, Rayan Hussein, Steven Miller, and A. Pouyan Nejadhashemi

***Abstract*—Many societal and industrial problem-solving tasks involving search, optimization, design and management are conveniently decomposed into hierarchical sub-problems. While this process allows a systematic procedure to have a multistakeholder solution, the independent decision-making process for the lower-level problem causes a deviation in the expected outcome of the upper-level problem. In this paper, we provide a new and computationally efficient evolutionary approach allowing upper-level decision-makers to analyze the vagaries of lower-level decision-making when choosing a preferred solution with the minimum deviation from their expectations. This concept is novel and pragmatic. We demonstrate the concept through a search for optimistic-pessimistic trade-off solutions found by an evolutionary multi-objective optimization approach first on two difficult test problems, then on a watershed management problem and a telecommunication management problem. The approach is generic and can be applied to similar hierarchical management problems to achieve minimum deviation with a more predictive and reliable outcome. The proposed solution procedure is found to choose an optimistic solution that has approximately 31% to 65% reduced deviation compared to another optimistic solution chosen at random in the test problems and approximately 85% to 95% reduced deviation in the two practical problems, making the method of this study applicable to practical hierarchical problems.**

***Index Terms*—Hierarchical optimization, decision-making, evolutionary algorithms, bi-level optimization.**

I. Introduction

MANY societal and industrial management problems involve multiple levels of a hierarchy, mainly due to the ease of managing and controlling various aspects of the problems (for example, see [1], [2], [3] for algorithms and [4], [5] for applications). Each level may involve an optimization sub-problem with certain decision variables, constraints and objectives, which are dictated and controlled by a set of users or decision-makers (DMs). In their simplest form, there can be two levels – an upper level (UL) and a lower level (LL). The variables of both levels are usually non-overlapping and controlled by the DMs of the respective level. However, the sub-problems are linked, and each level requires a combination of UL and LL variables to compute its respective objective and constraint values. Due to the existence of two different independent groups of DMs and the complexity involved in the interconnection of the two sub-problems, an implementation of a theoretical UL Pareto-optimal solution does not often produce the desired objective outcome [6], a matter that has been discussed well from the perspective of socioeconomic theories [7], [8], [9], [10]. While the usual causes of difficulties, such as problems being nonlinear and non-stationary over time, having the presence of uncertain parameters and variables, and being diluted with personal gains and deceits, are very much in play, we here address a solvable issue in which the preferences of two distinct but hierarchical groups of DMs (e.g., government policy-makers at the UL and end-users at the LL) can be analyzed to identify a solution that accounts for the minimum possible deviation in the UL's outcome due to alternate choices available for the LL.

The authors are from College of Engineering and College of Agricultural and Natural Sciences of Michigan State University, East Lansing, MI, 48824 USA. Corresponding author's e-mail: (kdeb@msu.edu).

Consider, for example, a watershed management problem in which the upper-level decision-makers (UL-DMs) are government policy-makers who determine the set of Best Management Practices (BMPs) for granting subsidies (UL variables) to local farmers (LL-DMs) with a goal of minimizing the delivery of pollutants (e.g., nutrients, sediments) to water bodies while minimizing the investment in restoration plans. Thus, the UL problem itself may involve more than one objective to find a practically viable solution. Meanwhile, the LL-DMs must decide which particular BMPs to implement on their land (LL variables) for multiple objectives: maximize their own profits and long-term benefits. Clearly, both the UL and LL objectives are dependent on the subsidized BMPs (UL variables) fixed by the UL-DMs and the spatial allocation of the BMPs (LL variables) fixed by the LL-DMs. In this problem, two sub-problems are hierarchically linked through the effects of BMP implementation on nearby streams' water quality. The overall BMP implementation cost is controlled by the UL-DMs and its spatial allocation is determined by the LL-DMs. While farmers can indirectly force policy-makers to change their BMP policies to achieve a better economic-environmental trade-off, policy-makers exert a direct effect in forcing farmers to choose BMPs that are beneficial to the farmers and the policy-makers. Thus, UL-DMs wield greater influence in determining the outcome of the overall process, but do not have complete control in determining the final outcome, causing a variation in their expected[1] outcome (objective and constraint values) due to the independence of decision-making at the LL. This aspect makes hierarchical problems different and more challenging from an implementation point of view than single-level problems.

By considering the optimization problem at each level, we see that due to the multiple conflicting objectives, it is likely that there will be multiple trade-off (Pareto-optimal) solutions at each level. For example, for the above watershed management problem, farmers can define a specific BMP spatial allocation based on the set of prioritized BMPs provided by governmental policy makers, producing a set of solutions trading off their profit and long-term benefits. It is clear that LL-DMs have complete liberty to choose a single preferred solution from among their own trade-off solutions without considering or consulting with the UL-DMs. However, as evident from the above discussions, their trade-off solutions are clearly controlled by the UL-DMs.

On the other hand, while the UL-DMs can choose their own preferred solution from the UL trade-off solution (Pareto) set, unfortunately, the trade-off set depends on what has been chosen by the LL-DMs. For example, the total BMP implementation cost and the generated pollutant loads (UL objectives) cannot be computed exactly unless the policy-makers know which BMPs were selected by the farmers (LL-DMs) and where they were placed within the watershed. If UL-DMs have the liberty to decide for the LL-DMs, they can take full control of solving the complete problem and find the best possible trade-off set for their own objectives. Such idealistic solutions are called *optimistic* solutions in the bi-level optimization literature [11]. Due to the full access of the objectives and constraints of both levels available to UL-DMs, UL-DMs can simulate the whole process and find the respective optimistic solution set. It is clear that optimistic solutions are theoretical and represent the best trade-off of UL objectives that UL-DMs can ever expect, but may not be possible to achieve them in reality. This is because farmers (LL-DMs) are independent entities and may not choose the exact optimal water quality policy associated with the optimistic solutions found optimal by governmental policy-makers (UL-DMs). Importantly, the farmers' independent preferred solution may not lead to the most cost-effective solution at the UL. The independence of LL-DMs will cause a deviation between the outcome involving UL objective values and the UL-DM's desired values.

Under this scenario, we propose a pragmatic solution methodology that can lead to a good compromise and predictable solution for the UL-DMs. Instead of choosing a preferred solution from the optimistic trade-off set (which is computable but theoretical), UL-DMs may choose a solution from their theoretical trade-off set that in reality results in a minimum expected deviation (MED) solution of all LL-controlled solutions (loosely associated with the so-called *pessimistic* solutions known in the bi-level literature [11]) from its optimistic objective values. We argue that by doing so, the UL-DMs can minimize the deviation of their expectation from the unknown choice in the LL decision-making process, and the resulting MED solution may turn out to be a practically well-predicted solution for implementation. However, from a computational perspective, finding the optimistic and pessimistic solutions for a bi-level optimization problem is a challenging task. The linkage between UL and LL variables and the associated complexities involved in computing multi-objective UL and LL problems makes the task even more difficult.

This paper proposes a systematic, computational decision-making procedure for obtaining a MED solution for a bi-level multi-objective scenario. First, it employs a bi-level evolutionary multi-objective optimization (BLEMO) algorithm [12] to find multiple Pareto-optimal solutions at both UL and LL levels simultaneously. Then, the obtained BLEMO solutions are analyzed to identify the MED solution by using four strategies proposed for the first time. It is evident that the evolutionary optimization approach makes the identification of the MED solution possible simply due to the flexible search used to find and store multiple alternate trade-off solutions in an implicit parallel manner. The key achievements of this paper are summarized as follows:

– In addition to reviewing the principles of a bi-level, multi-objective optimization problem, the paper clearly defines the optimistic Pareto-optimal solutions and suggests existing efficient evolutionary-based computational methods to find them.

– The paper also links the MED solution identification process through pessimistic solutions, which correspond to the maximum UL objective values for optimistic UL solutions due to their association with different LL Pareto-optimal solutions. However, pessimistic solutions are computationally challenging to find, involving a tri-level, multi-objective optimization problem, and may not be the right solutions to qualify as MED solutions for practical reasons.

– To reduce the computational complexity and to find practically more accurate MED solutions, we propose a two-step pseudo-pessimistic solution procedure in this paper for the first time.

– The paper finally proposes a simplistic and direct computational approach to first find an optimistic solution set and then propose a follow-up single UL-objective based bi-level optimization procedure to identify the MED solution.

– We demonstrate the working of the above approaches on two test problems and then presents results for two practical problems.

In the remainder of this paper, first, we provide the basics of bi-level problem formulation in Section II. We also define optimistic and pessimistic solution sets in the context of bi-level multi-objective problem-solving tasks and

[1] This is not an average outcome, but what to expect in reality.

introduce a computationally tractable pseudo-pessimistic solution set identification procedure. In Section III, we provide the motivation and approaches for the proposed study in choosing the preferred MED solution using a bi-level multi-objective decision-making approach. The proof-of-principle results on two numerical test problems are presented in Section IV. Then, the results on two real-world problems – a watershed management problem and a telecommunication management problem – are presented in Sections V and VI, respectively. Finally, conclusions and future studies are discussed in Section VII.

II. Hierarchical Problem Solving Tasks

Without loss of generality, we consider two-level hierarchical optimization problems in this paper, but the concept can be extended to more than two levels as well. In a bi-level optimization problem, there exist two sets of variables $\mathbf{x}$ ($\in \mathbb{R}^N$), explicitly varied in the upper-level (UL) problem, and $\mathbf{y}$ ($\in \mathbb{R}^n$), explicitly varied in the lower-level (LL) problem. For a specific UL-variable vector $\bar{\mathbf{x}}$, as shown in Fig. 1, the LL constrained optimization problem (shown in the inset figure) is solved to find the Pareto-optimal LL solutions, such as $\mathbf{y}^*_{\bar{\mathbf{x}}}$. In this LL optimization task, the UL-variable vector $\bar{\mathbf{x}}$ is kept fixed. The combination $(\bar{\mathbf{x}}, \mathbf{y}^*_{\bar{\mathbf{x}}})$ is then evaluated at the UL for its objective and constraint values. Thus, in a sense, the replacement of $\mathbf{y}$ with the LL-optimal solution $\mathbf{y}^*$ becomes a mandatory constraint at the UL. The UL optimization eventually finds the UL optimal solution $\mathbf{x}^*_p$ with its associated LL optimal solution(s) $\mathbf{y}^*_p$, making $(\mathbf{x}^*_p, \mathbf{y}^*_p)$ one of the Pareto-optimal solutions of the overall bi-level optimization problem (see [13], [14] for certain recent algorithms). Due to the widespread existence of bi-level problems in practice, an increasing number of application studies are emerging on the topic [15], [16], [17], [18].

A. Bi-level Multi-objective Optimization Problem (BLMOP)

In the presence of multiple objectives at each level, the following definition presents a bi-level multi-objective optimization problem.

Definition 1: For the upper-level objective vector $\mathbf{F} : \mathbb{R}^N \times \mathbb{R}^n \rightarrow \mathbb{R}^M$ and lower-level objective vector $\mathbf{f} : \mathbb{R}^N \times \mathbb{R}^n \rightarrow \mathbb{R}^m$, the bi-level multi-objective optimization problem (BLMOP) is given as follows:

$$\begin{aligned}
\underset{\mathbf{x}\in\mathbf{X},\mathbf{y}\in\mathbf{Y}}{\text{Minimize}}\ & \mathbf{F}(\mathbf{x},\mathbf{y}) = (F_1(\mathbf{x},\mathbf{y}),\ldots,F_M(\mathbf{x},\mathbf{y})),\\
\text{subject to}\ & \mathbf{y} \in \underset{\mathbf{y}\in\mathbf{Y}}{\operatorname{argmin}}\{\mathbf{f}(\mathbf{x},\mathbf{y}) = (f_1(\mathbf{x},\mathbf{y}),\ldots,f_m(\mathbf{x},\mathbf{y}))\big|\\
& \qquad g_j(\mathbf{x},\mathbf{y}) \le 0,\quad j=1,\ldots,c\},\\
& G_k(\mathbf{x},\mathbf{y}) \le 0,\quad k=1,\ldots,C,
\end{aligned} \tag{1}$$

where $G_k : \mathbb{R}^N \times \mathbb{R}^n \rightarrow \mathbb{R}$, $k = 1,\ldots,C$, denotes the k-th upper level constraint and $g_j : \mathbb{R}^N \times \mathbb{R}^n \rightarrow \mathbb{R}$, $j = 1,\ldots,c$, denotes the j-th lower level constraint. Any variable bound in $\mathbf{x} \in \mathbf{X}$ and $\mathbf{y} \in \mathbf{Y}$ is treated within the respective inequality constraint set. Equality constraints may also exist but are avoided here for brevity.

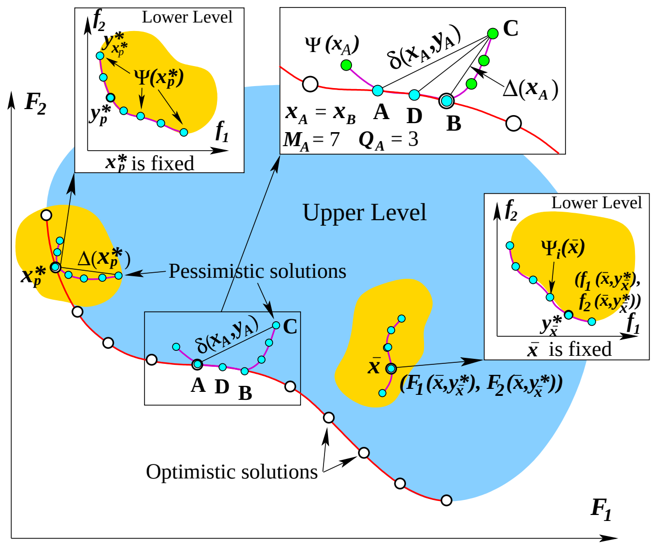

Fig. 1. UL Pareto-optimal front and LL Pareto-optimal fronts for a few bi-level solutions. A mapping of the entire lower-level feasible space is shown in the UL objective space.

Definition 2: Let $\Psi(\mathbf{x})$ be a set of LL Pareto-optimal solution vectors for a given UL solution vector $\mathbf{x}$ with $\Psi_i(\mathbf{x}) : \mathbb{R}^N \rightarrow \mathbb{R}^n$:

$$\begin{aligned}
\Psi(\mathbf{x}) = \underset{\mathbf{y}\in\mathbf{Y}}{\operatorname{argmin}}\{&\mathbf{f}(\mathbf{x},\mathbf{y}) = (f_1(\mathbf{x},\mathbf{y}),\ldots,f_m(\mathbf{x},\mathbf{y}))\big|\\
& g_j(\mathbf{x},\mathbf{y}) \le 0,\quad j=1,\ldots,c\}.
\end{aligned} \tag{2}$$

The exact number of LL Pareto-optimal solutions for any given $\mathbf{x}$ can be from one to infinity. Fig. 1 shows a sketch of a UL variable vector $\bar{\mathbf{x}}$ in the UL objective space and the respective LL objective space for which $\Psi_i(\bar{\mathbf{x}})$ is one of many LL optimal solutions. The LL feasible objective space and respective Pareto-optimal solutions are mapped to the UL objective space. It is interesting that although there may exist feasible but non-Pareto LL solutions that may produce better UL objective vectors than the UL Pareto front (as shown by the yellow extended region for $\mathbf{x}^*_p$ in the figure), because they are not Pareto-optimal at the LL, they will be considered infeasible at the UL. The BLMOP described in Equation 1 can be rewritten as follows:

$$\begin{aligned}
\underset{\mathbf{x}\in\mathbf{X},\mathbf{y}\in\mathbf{Y}}{\text{Minimize}}\ & F(\mathbf{x},\mathbf{y}) = (F_1(\mathbf{x},\mathbf{y}),\ldots,F_M(\mathbf{x},\mathbf{y})),\\
\text{subject to}\ & \mathbf{y} \in \Psi(\mathbf{x}),\\
& G_k(\mathbf{x},\mathbf{y}) \le 0,\quad k=1,\ldots,C.
\end{aligned} \tag{3}$$

Due to multi-objective nature of the problem, it is expected that there will be multiple Pareto-optimal solutions for the above problem. Let one of them be $(\mathbf{x}^*_p, \mathbf{y}^*_p)$. For a specific UL vector $\mathbf{x}^*_p$, there can be a single LL Pareto-optimal solution $\mathbf{y}^*_p$, or there can be a set of multiple LL Pareto-optimal solutions $\Psi(\mathbf{x}^*_p)$, among which a few may belong to the bi-level optimal solution set $\mathbf{y}^*_p \in \Psi(\mathbf{x}^*_p)$. When there are multiple lower-level optimal solutions for a specific UL vector $\mathbf{x}_p^*$, it is not clear which member(s) of $\Psi(\mathbf{x}_p^*)$ will correspond to the bi-level optimal set. One way to resolve this issue is to find and pass all optimal LL solutions $\Psi(\mathbf{x}_p^*)$ to the UL for it to sort out the non-dominated solutions.

B. BLEMO Algorithm

In the problems of interest, both the UL and LL problems involve multiple conflicting objectives, thereby requiring multiple Pareto-optimal solutions to be found at both levels. Moreover, the UL Pareto-optimal solutions are associated with one or more LL Pareto-optimal solutions that make the overall solutions optimal at the UL. Here, we use a previously proposed BLEMO algorithm [12]. BLEMO uses a few generations of the NSGA-II procedure at the LL for every UL solution. The resulting LL non-dominated (ND) solutions of each UL solution are then processed at the UL to update UL solutions using another NSGA-II procedure applied at the UL. This interconnected dual NSGA-II procedure is continued until a termination criterion is satisfied. The UL NSGA-II chooses the appropriate LL ND solutions for each UL solution to keep the overall optimization process focused on arriving at UL Pareto-optimal solutions. The formulations provided in Sections III-A to III-D can be directly used to find the targeted solution, but special care needs to be taken to find and maintain a diverse set of solutions at the UL.

C. Optimistic Solutions

Every solution of the problem defined in Equation 1 or 3 is referred to as an optimistic solution ($(\mathbf{x}_p^*, \mathbf{y}_p^*)$). The emphasis is on finding multiple optimistic trade-off solutions that will optimize the bi-level problem with good diversity. This means that the goal is to find a finite set of P UL optimal variable vectors $\{\mathbf{x}_p^*\}$ for $p = 1, \ldots, P$ and their associated finite (say, with at most Q_p members) LL optimal variable vector set ($\mathbf{y}_{p,q}^* \in \Psi(\mathbf{x}_p^*)$, for $q = 1, 2, \ldots, Q_p$) that minimizes all M UL objectives ($\mathbf{F}$) and satisfies all UL and LL constraints (refer to Fig. 1). Because a finite set of trade-off optimistic solutions are to be found, it is expected that they will maintain a good diversity in terms of their UL objective values to facilitate better decision-making in the end.

As discussed above, for each UL vector $\mathbf{x}_p^*$ in the bi-level Pareto-optimal set, there may exist a number of LL optimal variable vectors (the set $\Psi(\mathbf{x}_p^*)$). Say there are M_p (equal to the number of LL vectors in $\Psi(\mathbf{x}_p^*)$) LL optimal solutions for $\mathbf{x}_p^*$ in the set, but not all combinations $(\mathbf{x}_p^*, \Psi_i(\mathbf{x}_p^*))$ for $i = 1, 2 \ldots, M_p$ may be present in the optimistic solution set. The inset sketch in Fig. 1 illustrates a scenario with $M_p = 7$ combinations. Many of the combinations (such as point C in the inset figure) will be dominated by other optimistic Pareto-optimal solutions (such as point B), as shown in Fig. 1. Let us denote $I(\mathbf{x}_p^*)$ of size Q_p as the set of indices of $\Psi(\mathbf{x}_p^*)$ that corresponds to Pareto-optimal (optimistic) solutions of the BLMOP with a specific UL variable vector $\mathbf{x}_p^*$. Note that if $Q_p = |I(\mathbf{x}_p^*)| = 1$ (as in the solution marked by $\mathbf{x}_p^*$ in the figure), then the UL variable vector $\mathbf{x}_p^*$ occurs only once in the entire optimistic set; otherwise, it occurs multiple times (as with the solutions marked as A, B, and D, which share the same $\mathbf{x}^*$ vector). Thus, a bi-level optimistic solution to the BLMOP can be represented as a combination of the UL solution $\mathbf{x}_p^*$ and one of its associated Q_p LL optimal solutions $\Psi_i(\mathbf{x}_p^*)$ (for $i \in I(\mathbf{x}_p^*)$), or $\mathbf{s}_{p,i}^{\text{opt}} = (\mathbf{x}_p^*, \Psi_i(\mathbf{x}_p^*))$ involving the i-th LL optimal solution. The respective UL objective vector is $\mathbf{F}(\mathbf{s}_{p,i}^{\text{opt}})$. The $\mathbf{x}^*$ vector resulting in seven points in the inset figure has $Q_p = 3$ such occurrences (A, D, and B) in its LL Pareto-optimal set.

The complexity of the outcome of the BLMOP requires an efficient and population-based optimization algorithm [12] to be employed.

III. Decision-Making in BLMOP

There is a practical aspect that changes the way the optimal solutions must be viewed for a multi-objective bi-level problem. If all LL optimal solutions ($\Psi(\mathbf{x})$) are not passed to the UL for evaluation, and instead a few preferred LL-optimal solutions are sent, the optimistic solutions may not be achievable at the UL. In Fig. 1, if the LL solution marked as $\mathbf{y}_p^*$ is missed by the LL optimization algorithm, or is not considered to be important by the LL-DMs and hence was not allowed to be considered by the UL-DMs, then the optimistic Pareto-optimal front will not have $\mathbf{x}_p^*$ as a possible solution to the bi-level problem. Thus, the optimistic solutions to a bi-level problem can theoretically achieve the best possible UL solutions ($\mathbf{x}^*$) with the optimal UL objective values ($\mathbf{F}^{\text{opt}}$) for the underlying problem, but due to the practicality of having an independent group of DMs at the LL, the UL-DMs may never achieve the same optimistic UL objective values ($\mathbf{F}^{\text{opt}}$) in reality. This causes a deviation from the expected outcome at the UL.

Let us define a normalized deviation metric $\delta(\mathbf{x}_p^*, \mathbf{y}_p^*)$ for computing the maximum difference in the normalized UL objective vectors ($\widehat{\mathbf{F}}$) of a specific UL optimistic solution $\mathbf{x}_p^*$ from all LL optimal solutions $\mathbf{y}_p^* \in \Psi(\mathbf{x}_p^*)$, as follows:

$$\delta(\mathbf{x}_p^*, \mathbf{y}_p^*) = \max_{i=1}^{M_p} \left\| \widehat{\mathbf{F}}(\mathbf{x}_p^*, \Psi_i(\mathbf{x}_p^*)) - \widehat{\mathbf{F}}(\mathbf{x}_p^*, \mathbf{y}_p^*) \right\|, \quad (4)$$

where the normalized $\widehat{F}_j$ (for $j = 1, \ldots, M$) vectors are computed using minimum and maximum values in the trade-off set, as follows:

$$\widehat{F}_j(\mathbf{x}, \mathbf{y}) = \frac{F_j(\mathbf{x}, \mathbf{y}) - F_j^{\min}}{F_j^{\max} - F_j^{\min}}, \quad (5)$$

where $F_j^{\min} = \min_{p=1}^{P} \min_{i \in I(\mathbf{x}_p^*)} F_j\big(\mathbf{x}_p^*, \Psi_i(\mathbf{x}_p^*)\big)$, and $F_j^{\max} = \max_{p=1}^{P} \max_{i \in I(\mathbf{x}_p^*)} F_j\big(\mathbf{x}_p^*, \Psi_i(\mathbf{x}_p^*)\big)$. For $Q_p = |I(\mathbf{x}_p^*)| > 1$ (such as points A, B, and D in Fig. 1), the above metric computes the maximum deviation of all $I(\mathbf{x}_p^*)$-indexed LL variable vectors. Points A, B and D in Fig. 1 share the same $\mathbf{x}$: $\mathbf{x}_D = \mathbf{x}_B = \mathbf{x}_A$. The normalized deviation metric $\delta(\mathbf{x}_A, \mathbf{y}_A)$ for the UL variable vector $\mathbf{x}_A$ occurs for the LL variable vector for point C, having the largest normalized Euclidean distance from A to all $\Psi(\mathbf{x})$ points in the UL objective space. Using the above metric, we can now define an overall deviation metric that computes the minimum δ of all LL variable vectors in $I(\mathbf{x}_p^*)$ for a UL optimistic solution vector $\mathbf{x}_p^*$, as follows:

$$\Delta(\mathbf{x}_p^*) = \min_{\mathbf{y}_p^* \in \{\Psi_i(\mathbf{x}_p^*) \mid i \in I(\mathbf{x}_p^*)\}} \delta(\mathbf{x}_p^*, \mathbf{y}_p^*). \quad (6)$$

Let us denote the respective LL variable vector with $\mathbf{y}^*_{\mathbf{x}_p^*}$ corresponding to the minimum $\Delta(\mathbf{x}_p^*)$. For $\mathbf{x}_A$ in the figure, this corresponds to the Euclidean distance between B and C, marked in the figure, satisfying $\mathbf{y}^*_{\mathbf{x}_p^*} = \mathbf{y}_B$. Additionally, for the point $\mathbf{x}_p^*$ marked in the figure, there is a single element in $I(\mathbf{x}_p^*)$ and the respective Δ-metric value is also shown. Finally, for all P UL variable vectors in the bi-level Pareto-optimal set, the UL-DMs have a convenient way to choose a single preferred solution $\mathbf{x}^{\text{pref}}$ having the minimum deviation Δ:

$$\mathbf{x}^{\text{pref}} = \text{argmin}_{p=1}^{P} \Delta(\mathbf{x}_p^*). \quad (7)$$

The overall preferred solution is $(\mathbf{x}^{\text{pref}}, \mathbf{y}^*_{\mathbf{x}^{\text{pref}}})$.

A. Computational Procedure for Finding a Minimum Expected Deviation (MED) Solution: The Naive Approach

Based on the above discussions, we here outline the computational procedure of the proposed Naive Minimum Expected Deviation (N-MED) principle for bi-level hierarchical problems:

- Step 1: Find multiple optimistic trade-off solutions $\mathbf{s}_p^{\text{opt}} = (\mathbf{x}_p^*, \mathbf{y}_p^*)$ $(p = 1, \ldots, P)$ for the bi-level problem formulated in Equation 1. Note that $\mathbf{y}_p^*$ can be a set of LL variable vectors ($\Psi_i(\mathbf{x}_p^*)$ with indices specified in $i \in I(\mathbf{x}_p^*)$).
- Step 2: For each distinct $\mathbf{x}_p^*$, record multiple LL trade-off solutions $\Psi(\mathbf{x}_p^*)$ of which $\mathbf{y}_p^*$ is a member. This makes the approach naive.
- Step 3: For each distinct $\mathbf{x}_p^*$, compute the minimum deviation $\Delta(\mathbf{x}_p^*)$ using Equation 6, and then choose the UL variable vector $\mathbf{x}^{\text{pref}}$ to construct the preferred solution ($\mathbf{s}^{\text{N-MED}} = (\mathbf{x}^{\text{pref}}, \mathbf{y}^*_{\mathbf{x}^{\text{pref}}})$) for the BLMOP using Equation 7.

The above naive procedure requires us to compute and record all (or a finite set of) LL variable vectors $\Psi(\mathbf{x}_p^*)$ for every UL variable vector $\mathbf{x}_p^*$ in Step 2. An alternate procedure is to directly find $\Psi(\mathbf{x}_p^*)$ vectors that correspond to $\mathbf{y}^*_{\mathbf{x}_p^*}$ for each $\mathbf{x}_p^*$. The following optimality principle in the context of bi-level optimization allows such a computational procedure.

B. Pessimistic Solution Approach

An extreme case of optimistic solutions is to define pessimistic solutions. Pessimistic solutions correspond to the front that is maximally deviated from the optimistic front; thus, it may be important to find them to help provide an idea of the maximum deviation in the expected outcome of UL objective values due to the unknown decision-making on the part of LL-DMs. The resulting optimization problem to find the pessimistic solutions becomes a tri-level (min-max-min) optimization problem [11], as follows:

$$\begin{aligned}
\underset{\mathbf{x}\in\mathbf{X}, \mathbf{y}\in\Psi^P(\mathbf{x})}{\text{Minimize}} \quad & \mathbf{F}(\mathbf{x},\mathbf{y}) = \big(F_1(\mathbf{x},\mathbf{y}), \ldots, F_M(\mathbf{x},\mathbf{y})\big), \\
\text{subject to} \quad & \Psi^P(\mathbf{x}) \in \underset{\mathbf{y}\in\Psi(\mathbf{x})}{\text{argmax}} \Big\{ \big(F_1(\mathbf{x},\mathbf{y}), \ldots, F_M(\mathbf{x},\mathbf{y})\big) \Big| \\
& \quad \Psi(\mathbf{x}) \in \underset{\mathbf{y}\in\mathbf{Y}}{\text{argmin}} \big\{ \big(f_1(\mathbf{x},\mathbf{y}), \ldots, f_m(\mathbf{x},\mathbf{y})\big) \big| \\
& \quad g_j(\mathbf{x},\mathbf{y}) \leq 0, \quad j = 1, \ldots, c \big\}, \\
& G_k(\mathbf{x},\mathbf{y}) \leq 0, \quad k = 1, \ldots, C \Big\}.
\end{aligned} \quad (8)$$

For every UL variable vector $\mathbf{x}$, all LL variable vectors $\mathbf{y} \in \Psi(\mathbf{x})$ that minimize the LL problem are first found by solving the inner-most problem. Thereafter, the intermediate-level problem is solved to find LL variable vectors ($\mathbf{y}$) that maximize the UL objectives with the UL constraints. Since the obtained set $\Psi^P(\mathbf{x})$ is a subset of $\Psi(\mathbf{x})$, two levels (the second and third levels) of optimization are needed to obtain $\Psi^P(\mathbf{x})$. The feasible combined vectors $(\mathbf{x}, \Psi_i^P(\mathbf{x}))$ ($\mathbf{x}$ with each pessimistic LL vector $\Psi_i^P(\mathbf{x})$) are then evaluated at the upper-most level to minimize the UL objective functions to obtain the pessimistic solution set $(\mathbf{x}_j^{\text{pess}}, \mathbf{y}_j^{\text{pess}})$ for $j = 1, 2, \ldots$. The sets of optimistic (obtained by solving Equation 1) and pessimistic UL objective vectors are used to find the specific pair of optimistic and pessimistic solutions having the shortest Euclidean distance between them. Then, the respective optimistic solution is chosen as the $\mathbf{s}^{\text{P-MED}}$ solution. Fig. 2 illustrates a set of optimistic and pessimistic solutions in the UL objective space and the $\mathbf{s}^{\text{P-MED}} = (\mathbf{x}_3, \mathbf{y}_3)$ solution having the shortest Euclidean distance between the two sets. Note that Equations 4 to 7 are not used for

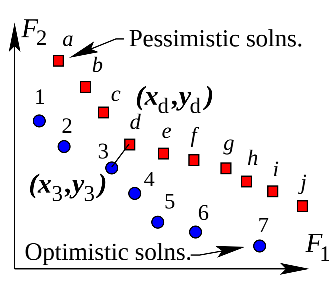

Fig. 2. Pessimistic approach used to identify the $\mathbf{s}^{\text{P-MED}}$ solution (#3).

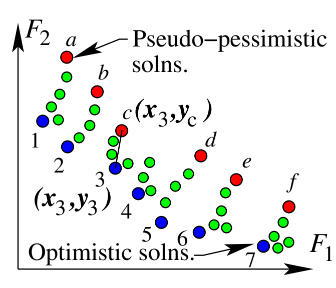

Fig. 3. Pseudo-pessimistic approach used to find the $\mathbf{s}^{\text{PP-MED}}$ solution (#3).

finding this pessimistic solution. Fig. 1 shows two likely pessimistic solutions originating from two optimistic UL variable vectors, but whether they truly belong to the pessimistic front will depend on the pessimistic solutions originating from other optimistic solutions.

We do not recommend the use of the pessimistic solutions for our purposes because of two difficulties. First, a tri-level problem is more complex to solve than a bi-level problem. Second, the hierarchical structure of the decision-making in a BLMOP dictates that UL-DMs will choose and announce their preferred solution first, before the LL-DMs have a chance to choose their most preferred solution from among the respective LL Pareto-optimal solutions. Hence the tri-level approach may produce UL solutions that are different from the true bi-level solutions of the original problem defined in Equation 1. Thus, the pessimistic solutions may be inappropriate for identifying the MED solution because of implementational difficulty. Next, we propose a two-stage method that is more appropriate and computationally appealing for our purpose.

C. Pseudo-Pessimistic Solution Approach

First, the optimistic UL variable vectors ($\mathbf{x}_p^*, p = 1,\ldots,P$) and respective optimal UL objective values $\mathbf{F}^{\rm opt}$ are found by solving the bi-level problem defined in Equation 1. Next, the following bi-level optimization problem is solved to find the pseudo-pessimistic solutions by restricting the UL variable vectors to be confined to the $\mathbf{x}_p^*$ set, as follows:

$$\begin{array}{rl}\underset{\mathbf{x}\in\{\mathbf{x}_p^*\},\mathbf{y}\in\mathbf{Y}}{\text{Maximize}} & \mathbf{F}(\mathbf{x},\mathbf{y}) = \left(F_1(\mathbf{x},\mathbf{y}),\ldots,F_M(\mathbf{x},\mathbf{y})\right),\\ \text{subject to} & \mathbf{y} \in \underset{\mathbf{y}\in\mathbf{Y}}{\text{argmin}}\{\mathbf{f}(\mathbf{x},\mathbf{y}) = \left(f_1(\mathbf{x},\mathbf{y}),\ldots,f_m(\mathbf{x},\mathbf{y})\right) \mid \\ & \qquad g_j(\mathbf{x},\mathbf{y}) \le 0, \quad j = 1,\ldots,c\},\\ & G_k(\mathbf{x},\mathbf{y}) \le 0, \quad k = 1,\ldots,C.\end{array} \tag{9}$$

The above problem restricts its UL search to all $\mathbf{x}_p^*$ solutions found by solving Equation 1 and finds associated LL solutions ($\mathbf{y}_p^{\rm p-pess}$) that maximizes the $\mathbf{F}$-vector, rather than minimizing it. Since $\mathbf{x}$ values are restricted to those corresponding to the optimistic solutions, the resulting bi-level solution set of the above problem corresponds to the original candidate LL solutions for computing MED values, but a different LL solution $\mathbf{y}_p^{\rm p-pess} \in \Psi(\mathbf{x}_p^*)$ than $\mathbf{y}_p^*$ is now obtained. As in the pessimistic case, the two sets (optimistic and pseudo-pessimistic) are used to identify the specific optimistic solution ($\mathbf{s}^{\rm PP\text{-}MED}$) having the shortest Euclidean distance from the pseudo-pessimistic solution set ($\mathbf{s}^{\rm PP\text{-}MED} = (\mathbf{x}_3, \mathbf{y}_3)$ in Fig. 3 has the shortest distance from the pseudo-pessimistic set). Note that some $\mathbf{x}_p^*$, such as $\mathbf{x}_4$ in the figure, may not have a representative $\mathbf{y}_4^{\rm p-pess}$, as all three $(\mathbf{x}_4, \Psi_i(\mathbf{x}_4))$ solutions are dominated by $(\mathbf{x}_5, \mathbf{y}_d)$. The two pessimistic solutions marked in Fig. 1 are also pseudo-pessimistic solutions.

The difference between the pessimistic and pseudo-pessimistic approaches is that the UL variable vectors for the pseudo-pessimistic approach are always a subset of the UL variable vectors of the optimistic set (in Fig. 3, $\mathbf{x}_c = \mathbf{x}_3$), while in the pessimistic approach, UL variable vectors other than those in the optimistic set can result (in Fig. 2, $\mathbf{x}_d$ may not even be present in the optimistic set). This aspect makes the pseudo-pessimistic approach more pragmatic, as the minimum deviation metric must be computed because of a change in LL variable vectors only and not because of a change in both UL and LL variable vectors to make the approach practical.

D. Direct MED (D-MED) Computational Approach

The N-MED approach restricts the identification of MED solution to the obtained finite set of $(\mathbf{x}_p^*, \mathbf{y}_p^*)$ solutions ($\mathbf{y}_p^* \in \Psi(\mathbf{x}_p^*)$). A more precise solution can be obtained by solving the following problem:

$$\begin{array}{rl}\underset{\mathbf{x}\in\{\mathbf{x}_p^*\},\mathbf{y}\in\mathbf{Y}}{\text{Minimize}} & \delta(\mathbf{x},\mathbf{y}) = \max_{i=1}^{M_p} \|\widehat{\mathbf{F}}(\mathbf{x}, \Psi_i(\mathbf{x})) - \widehat{\mathbf{F}}(\mathbf{x},\mathbf{y})\|,\\ \text{subject to} & \mathbf{y} \in \underset{\mathbf{y}\in\mathbf{Y}}{\text{argmin}}\{\mathbf{f}(\mathbf{x},\mathbf{y}) = \left(f_1(\mathbf{x},\mathbf{y}),\ldots,f_m(\mathbf{x},\mathbf{y})\right) \mid \\ & \qquad g_j(\mathbf{x},\mathbf{y}) \le 0, \quad j = 1,\ldots,c\},\\ & G_k(\mathbf{x},\mathbf{y}) \le 0, \quad k = 1,\ldots,C.\end{array} \tag{10}$$

The above formulation restricts the UL search to within the finite solution set $\{\mathbf{x}_p^*\}$ to identify $\mathbf{x}^{\rm dir}$ but finds a more precise variable vector $\mathbf{y}^{\rm dir}$ directly by using the minimum deviation expression in its upper-level objective function to obtain $\mathbf{s}^{\rm D\text{-}MED} = (\mathbf{x}^{\rm dir}, \mathbf{y}^{\rm dir})$.

The difference between D-MED and PP-MED solutions is that the deviation metric in the D-MED approach is always computed between an optimistic solution and another $\Psi(\mathbf{x}_p^*)$ driven solution for the same UL variable vector $\mathbf{x}_p^*$, and PP-MED (or P-MED) does not guarantee that. This aspect makes the D-MED approach the most practical. However, if precision in the LL variable vector is not an issue, the N-MED approach, which also restricts the deviation metric computation for the same UL variable vector, is the most computationally and practically viable approach.

E. Further Control in Decision-Making

It is clear that if all LL Pareto-optimal solutions ($\Psi(\mathbf{x}_p^*)$) for every UL Pareto-optimal ($\mathbf{x}_p^*$) solution are considered in the MED identification, both UL and LL decision-makers may lose control over introducing their preferences, and the process will find the best possible solution having the minimum expected deviation. However, if this is not desired and both UL-DMs and LL-DMs would like to influence the final solution to have certain preferences among their individual objectives, then δ (Equation 4), the Δ-metric (Equation 6) and the preference criterion (Equation 7) can be changed and made more problem-specific.

Two simple changes will allow both DMs to restrict the final MED solution to be within their predefined preference solution sets. First, a preference by LL-DMs can be implemented simply by redefining $\Psi(\mathbf{x}_p^*)$ to contain only the preferred LL solutions for $\mathbf{x}_p^*$. This will not allow any other non-preferred LL solutions to be considered for MED point identification. Second, Equation 7 can be applied only to preferred UL solutions ($\mathbf{x}_p^*$) instead of all P UL Pareto-optimal solutions.

A standard multi-criterion decision-making (MCDM) approach, such as the reference point method [19] or other methods [20], can also be used with a modified structure of Equations 4 to 7. For example, for a given aspiration point $\mathbf{z}$ and weight vector $\mathbf{w}$, the achievement scalarization function value ($\mathrm{ASF}(\mathbf{x}_p^*, \mathbf{y}_p^*, \mathbf{z}, \mathbf{w})$) of each optimistic solution ($\mathbf{x}_p^*, \mathbf{y}_p^*$) can be computed, and Equation 4 can be modified to the following:

$$\delta(\mathbf{x}_p^*, \mathbf{y}_p^*) = \mathrm{ASF}(\mathbf{x}_p^*, \mathbf{y}_p^*, \mathbf{z}, \mathbf{w}) \max_{i=1}^{M_p} \left\| \widehat{\mathbf{F}}(\mathbf{x}_p^*, \Psi_i(\mathbf{x}_p^*)) - \widehat{\mathbf{F}}(\mathbf{x}_p^*, \mathbf{y}_p^*) \right\|. \quad (11)$$

IV. Proof-of-Principle Results

We attempt to make the proposed approach more clear by first applying it to two bi-level test problems having two conflicting objectives at each level. In both problems, all objectives are minimized.

A. Test Problem DS1

The first problem is the DS1 problem [12], which has $N = n = 5$ UL and LL variables and $M = m = 2$ objectives in each level. The UL and LL objective functions are provided below.

$$\begin{cases} F_1(\mathbf{x}, \mathbf{y}) = & 1 + r - \cos(\alpha \pi x_1) + \sum_{j=2}^{n} (x_j - \frac{j-1}{2})^2 \\ & + \tau \sum_{i=2}^{n} (y_i - x_i)^2 - r \cos\left(\gamma \frac{\pi}{2} \frac{y_1}{x_1}\right), \\ F_2(\mathbf{x}, \mathbf{y}) = & 1 + r - \sin(\alpha \pi x_1) + \sum_{j=2}^{n} (x_j - \frac{j-1}{2})^2 \\ & + \tau \sum_{i=2}^{n} (y_i - x_i)^2 - r \sin\left(\gamma \frac{\pi}{2} \frac{y_1}{x_1}\right). \end{cases} \quad (12)$$

$$\begin{cases} f_1(\mathbf{x}, \mathbf{y}) = & y_1^2 + \sum_{i=2}^{n} (y_i - x_i)^2 \\ & + \sum_{i=2}^{n} 10(1 - \cos(\frac{\pi}{n}(y_i - x_i))), \\ f_2(\mathbf{x}, \mathbf{y}) = & \sum_{i=1}^{n} (y_i - x_i)^2 \\ & + \sum_{i=2}^{n} 10 |\sin(\frac{\pi}{n}(y_i - x_i))|. \end{cases} \quad (13)$$

The variable bounds are $x_1 \in [1, 4]$, $x_i \in [-n, n]$, for $i = 2, \ldots, n$ and $y_i \in [-n, n]$, for $i = 1, \ldots, n$. We consider $r = 0.3$, $\alpha = 1$, $\gamma = 1$, and $\tau = -1$ for this problem.

An analysis will reveal that the theoretical UL Pareto-optimal (optimistic) solutions correspond to $x_j^* = (j-1)/2$ for $j \geq 2$ and $x_1^* \in [2.0, 2.5]$. For a specific $\mathbf{x}^*$, the LL Pareto-optimal solutions occur at $y_j^* = x_j^*$ for $j \geq 2$ and $y_1^* \in [0, x_1^*]$. The LL y_1^* corresponding to the optimistic solution is $y_1^* = 2x_1^*(x_1^* - 2)$. However, we apply the BLEMO algorithm [12] to find $P = 100$ distinct optimistic solutions in Step 1 of the proposed N-MED approach using standard parameter settings [21], [22]. In Step 2, for each optimistic UL solution, $M_p = 20$ distinct LL trade-off solutions are obtained one by one. Finally, in Step 3, the optimistic solution corresponding to the minimum expected deviation metric Δ (Equation 7) is chosen as the preferred solution.

First, we show 100 optimistic UL trade-off solutions in Fig. 4 using blue shaded circles, obtained in Step 1. The trade-off between two UL objectives (F_1 and F_2) is clear from the figure. For the three x_1^* solutions, the respective

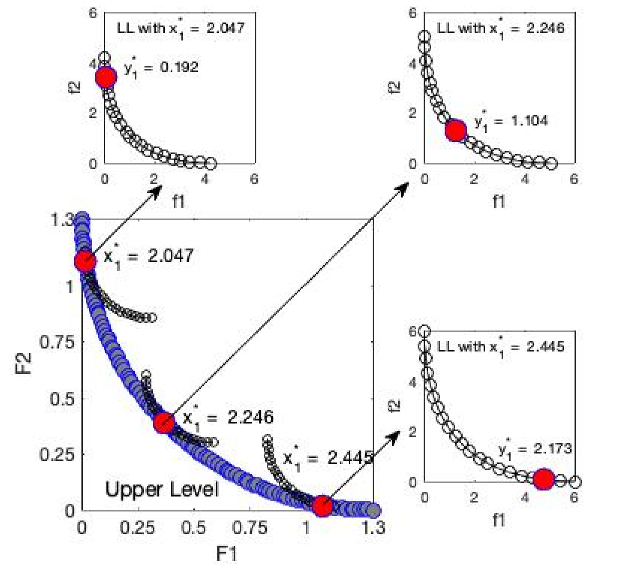

Fig. 4. UL optimistic solutions are shown in the UL objective space with optimal LL solutions for three x_1^* values.

LL Pareto-optimal solutions obtained in Step 2 are marked in the smaller offset figures. The y_1^* that corresponds to the optimistic solution is marked with a larger red circle. The other Pareto-optimal y_1 values, when mapped to the UL objective space, expand to a front, as shown in the main figure. Note that every x_1^* corresponds to a single y_1^* (with $Q_p = 1$), each of which comes from a different region in the respective LL Pareto-optimal set.

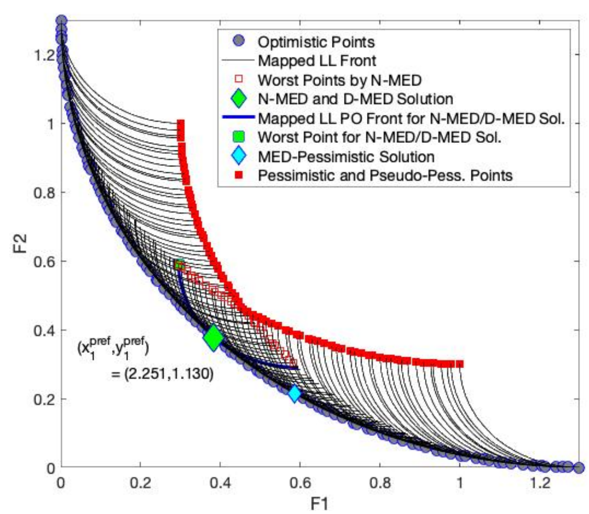

Fig. 5. Optimistic and pseudo-pessimistic solutions for the DS1 problem.

Fig. 5 plots the mapped LL solutions for each of the 100 UL solutions using a solid line. Thus, the solid lines in the figure indicate the effect of variation of the entire LL trade-off front for each UL solution in the UL objective space. In this problem, only one LL solution is Pareto-optimal at the UL level, and other LL solutions are dominated by it or other UL Pareto (optimistic) solutions. The worst mapped point is marked with a small red square for each optimistic UL solution. In Step 3, we find the preferred UL solution or N-MED ($\mathbf{s}^{\text{pref}}$, shown with a green diamond with $x_1^* = 2.251$ and $y_1^* = 1.130$), which minimizes the Δ-metric. The corresponding mapped LL trade-off front for $\mathbf{x}^{\text{pref}}$ is marked with a thick blue line, and the worst LL point is shown with a green square. Note that the same $\mathbf{s}^{\text{pref}}$ will result from the D-MED approach.

By choosing this preferred solution $\mathbf{x}^{\text{pref}}$, the UL-DMs ensure that despite not knowing which LL Pareto solution will be chosen by the LL-DMs, the deviation (along the thick blue line) from their expected optimistic UL objective values will be minimal. For this problem, the choice of the MED solution (with $\delta^* = 0.2305$) causes, on average, approximately 31% reduced deviation from another optimistic solution chosen at random ($\delta_{\text{avg}} = 0.3320$) and approximately 46% reduced deviation from the worst deviation ($\delta_{\max} = 0.4243$) possible. In this sense, the minimum deviation principle proposed in this paper can be considered an efficient decision-making principle for choosing a solution having the least deviation arising from the UL-DM's decisions.

Fig. 5 also shows the pessimistic or pseudo-pessimistic solutions for DS1 with filled red squares. Note that some of the worst points (open red squares) get dominated (in a maximization sense) by the other pseudo-pessimistic solutions (filled red squares). Note that for this problem, the pseudo-pessimistic points also correspond to pessimistic solutions. The front they indicate together shows the worst realized $\mathbf{F}$ values possible in choosing any optimistic solution. Thus, if pessimistic or pseudo-pessimistic solutions are used in Step 2 of the MED approach, the minimum Δ-metric solution (shown with a small cyan diamond) is found to be different ($x_1^* = 2.315$ and $y_1^* = 1.459$) than those found by the N-MED and D-MED approaches. Since the worst points for $\mathbf{x}^{\text{pref}}$ and its neighboring optimistic solutions are dominated and excluded from the Δ-metric computation, the resulting preferred solution obtained by using pessimistic or pseudo-pessimistic fronts is different and inferior for DS1. Thus, from a computational perspective, the two-phase D-MED method is attractive. Not only does it find the true MED solution, but it also does this with less computational effort than the pessimistic approach. Henceforth, we find the preferred solution using only the D-MED approach.

Before we leave DS1, we illustrate how the UL and LL DM's preferences can affect the identification of the N-MED/D-MED solution, as discussed in Section III-E. In Fig. 6, the UL-DM prefers the left one-third of the optimistic solutions, preferring F_1 more than F_2, and the LL-DM chooses the intermediate 50% of LL Pareto solutions rather than the complete LL front solutions.

B. Test Problem DS3

Problem DS3 produces an optimistic front having multiple LL-associated solutions for a single UL optimistic solution, unlike in DS1 in which every optimistic solution corresponded to a single LL solution. The DS3 problem description is given below:

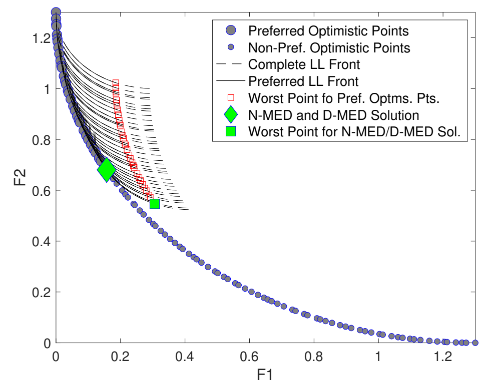

Fig. 6. N-MED/D-MED solution with preferred decision-making (discussed in Section III-E) for the DS1 problem.

$$\text{Minimize}\quad \mathbf{F}(\mathbf{x},\mathbf{y}) = \left\{ \begin{array}{c} x_1 + \sum_{j=3}^{N}(x_j - j/2)^2 + \tau\sum_{i=3}^{N}(x_i - y_i)^2 \\ -R(x_1)\cos\left(4\tan^{-1}\left(\frac{x_2-y_2}{x_1-y_1}\right)\right) \\ x_2 + \sum_{j=3}^{N}(x_j - j/2)^2 + \tau\sum_{i=3}^{N}(x_i - y_i)^2 \\ -R(x_1)\sin\left(4\tan^{-1}\left(\frac{x_2-y_2}{x_1-y_1}\right)\right) \end{array} \right\},$$

subject to

$$\begin{aligned} &\mathbf{y} \in \underset{(\mathbf{y})}{\text{argmin}} \left\{ \mathbf{f}(\mathbf{y}) = \begin{pmatrix} y_1 + \sum_{i=3}^{K}(y_i - x_i)^2 \\ y_2 + \sum_{i=3}^{K}(y_i - x_i)^2 \end{pmatrix} \middle| \right. \\ &\qquad \left. g(\mathbf{x},\mathbf{y}) = (y_1 - x_1)^2 + (y_2 - x_2)^2 \le r^2 \right\}, \\ &G(\mathbf{x}) = x_2 - (1 - x_1^2) \ge 0, \\ &0 \le x_j \le x^U, \text{ for } j = 1,\ldots,n \text{ and } x_1 \text{ is a multiple of 0.1}, \\ &-n \le y_i \le n, \quad \text{for } i = 1,\ldots,N. \end{aligned} \tag{14}$$

Here we use a periodically changing radius[2] $R(x_1) = 0.1 + 0.15|\cos(2\pi(y_1 - 0.12)|$ and set $r = 0.3$ and $x^U = 1.4$. We also set $N = n = 5$ for our illustration. For the upper-level Pareto-optimal solutions, $x_i^* = j/2$ for $j \ge 3$. The variables x_1^* and x_2^* take values satisfying the constraint $G(\mathbf{x}) = 0$. The variable x_1 takes discrete values, making the problem a discrete programming problem. In the range [0, 1.4] with a step of 0.1, there are 15 distinct values of x_1. For each $\mathbf{x}$, the LL Pareto solutions (y_1 and y_2) lie in the third quadrant of a circle with radius r and center at (x_1, x_2) in the $\mathbf{f}$-space. Additionally, $y_i^* = x_i^*$ for $i \ge 3$.

For this problem, it is difficult to find closed-form theoretical optimistic solutions. We employ the BLEMO algorithm [12] and find the optimistic solutions, which are shown in Fig. 7 with blue filled circles in Step 1 of the N-MED approach. The mapped LL Pareto-optimal front for a discrete set of $\mathbf{x}^*$ are shown with circles. Out of 15 possible x_1 discrete values, only 10 lie on the optimistic front and they dominate all points of the remaining five x_1 values (marked with dashed circles). The 20 LL Pareto-optimal solutions found in Step 2 are shown

[2] $R(x_1)$ is slightly modified from the original suggestion to make an intermediate x_1 the final preferred solution.

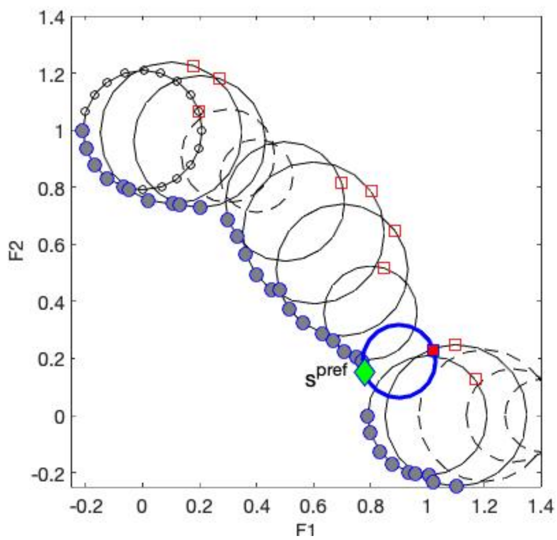

Fig. 7. Optimistic solutions and the resulting $\mathbf{x}^{\text{pref}}$ found by BLEMO are shown for the DS3 problem. The red filled circle is the LL solution for $\mathbf{s}^{\text{pref}}$.

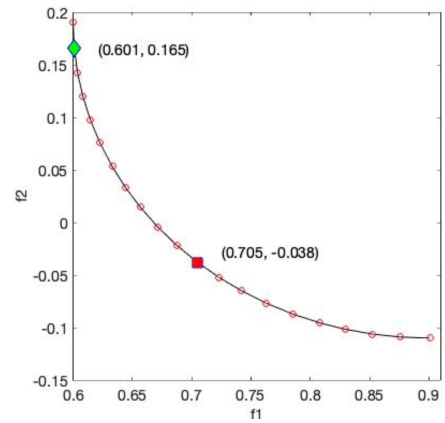

Fig. 8. The LL Pareto-optimal front and obtained trade-off solutions for $\mathbf{s}^{\text{pref}}$ are shown for the DS3 problem. The corresponding LL solution for $\mathbf{s}^{\text{pref}}$ and the worst point are also shown in filled diamonds and squares, respectively.

for $x_1^* = 0$. All LL Pareto-optimal solutions lie on the $g(\mathbf{x}, \mathbf{y}) = 0$ constraint in the LL variable space and satisfy $(f_1 - x_1)^2 + (f_2 - x_2)^2 = r^2$ for a given $\mathbf{x}$. When they are mapped to the UL objective space, they fall on a circle of radius $R(x_1)$ centered at (x_1, x_2). Unlike in DS1, in DS3, multiple optimistic solutions ($Q_p > 1$) occur for a single $\mathbf{x}^*$ vector. For example, for the left-most circle, five optimistic solutions share the same $\mathbf{x}^*$ vector as $x_1^* = 0$. Our proposed N-MED and D-MED approaches still work for such problems.

In Step 3, the worst LL Pareto-optimal solution (with maximum deviation in the UL objective space) is found using the proposed δ-metric (Equation 6) for every optimistic UL solution with a distinct x_1^*. Then, the maximum δ is computed for all optimistic solutions having the same x_1^* to obtain Δ. The respective worst points are marked with a red open square for 10 different x_1^* values. Finally, the optimistic solution having the minimum Δ is marked with a green diamond. The corresponding LL mapped front is shown with a thick blue circle with its worst point marked with a filled red square. This solution lies on the minimum-radius circle among the 10 different optimistic solutions. This preferred solution $\mathbf{s}^{\text{pref}}$ has $(x_1^*, x_2^*) = (0.900, 0.190)$ and respective $(y_1^*, y_2^*) = (0.601, 0.165)$. The respective LL Pareto front and trade-off solutions are shown in Fig. 8. For this problem, the choice of MED solution ($\delta^* = 0.0656$) causes, on average, approximately 65% reduced deviation from another optimistic solution chosen at random ($\delta_{\text{avg}} = 0.1862$) and approximately 74% reduced deviation from the worst deviation ($\delta_{\max} = 0.2476$) possible.

V. Watershed Management Problem

Conventional agricultural practices have greatly degraded the water quality of freshwater ecosystems around the world [23]. Excess nutrients and sediments have resulted in environmental problems such as eutrophication of inland and coastal waters, harmful algal blooms, habitat loss, and alterations in aquatic food chains [24], [25]. Excessive sediment delivery to surface waters is particularly insidious. Sediment deposition causes billions of dollars of damage a year, either through loss of crop productivity, energy production, and recreational value or through downstream mitigation measures such as dredging [26]. A primary option for sediment control is the implementation of BMPs at the source and upstream areas such as cropland. Some commonly used BMPs include no-till farming, cover crops, and filter strips [27]. Natural resource managers and policy-makers are generally interested in promoting these practices among farmers and land-owners in a cost-effective manner.

A. Problem Description

Remedying the environmental damage brought about by conventional agricultural management poses unique challenges to government agencies. Suppose a government entity seeks to ameliorate high levels of sediment loss in a watershed with a finite sum of money. One proven and effective option is to encourage farmers within the watershed to enact BMPs. However, numerous challenges lay in the method of implementing BMPs at the field level. First, since most BMPs entail some upfront cost (i.e., capital cost) and/or changes in agricultural yield, the majority of farmers must be incentivized to adopt BMPs through government subsidies. Second, there are a myriad of different BMPs to choose from, each with unique costs and environmental impacts. Finally, farmer behavior introduces a considerable lack of knowledge into BMP choice. Since BMP adoption is voluntary, governments will always face unpredictable rates of adoption of BMPs among farmers, as farmers have their own personal motivations and biases to decide on BMPs (e.g., change in revenue and changes in long-term benefits).

These challenges can be addressed through bi-level optimization by grouping the government and farmers into two distinct hierarchical levels. In this case, the state or local government is the UL-DM (i.e., watershed manager), who tries to choose the best BMP subsidies to offer with respect to total capital cost and environmental improvement. The farmers, on the other hand, are the LL-DMs, who either choose or refuse to adopt the government subsidies offered depending on their expected net revenue and change in agricultural yield per BMP implementation. Our proposed MED approach attempts to treat the problem as a hierarchical bi-level optimization problem and finds the MED solution using the proposed strategies.

B. Computational Procedure

Here we enact a real-world proof-of-concept scenario to illustrate the usefulness of the proposed bi-level decision-making procedure set within the Honeyoey Creek-Pine Creek watershed in Michigan, USA. We assume that a governmental agency chooses among 10 different BMPs, each with unique trade-offs between its cost of implementation and the effect of the reduction in sediment loading. The universal set of BMPs ($\mathbf{X}$) for this proof-of-concept are 'filter strips', 'tree & shrub establishment', 'vegetative barrier establishment', 'upland wildlife habitat management', 'integrated pest management', 'heavy use area protection', 'cover crop establishment', 'nutrient management', 'pumping plant installation', and 'water well installation'. The option of 'No-BMP' is the 11-th element of $\mathbf{X}$. Due to cost implications, the government agency (i.e., the UL-DM) decides to implement at most five of the 11 allowable BMPs. Thus, they must choose a subset ($\mathbf{x} = [x_1, x_2, x_3, x_4, x_5]$ where $x_i \in \mathbf{X}$) of the five BMPs to minimize the total costs of the accepted subsidies in dollars (F_c) and simultaneously minimize sediment loading in tons per day (F_s). The second UL objective (F_s) is calculated through the Soil and Water Assessment Tool (SWAT), which is a watershed-scale hydrologic model that, given topographic, soil, weather, land use, and agricultural management data, can predict the total sediment loading of the study area given the adoption patterns of the farmers on the LL [28].

The LL-DMs are the farmers in the study area who accept or reject the announced BMPs with the aims of maximizing the net revenue per BMP in dollars (f_r) and the long-term change in agricultural yield (f_o). To balance the computation time and accuracy of the optimization, we make two assumptions. First, we assume that all farmers grow one of the six common crops ('alfalfa', 'corn', 'sugar beets', 'soy beans', 'winter wheat', 'field peas') in the study area, making a six-variable LL decision vector $\mathbf{y}$ such that each $y_j \in \mathbf{x}$. Second, we assume that each farmer for a given crop acts as an individual decision maker, who either chooses a single BMP among the available BMPs from the UL or chooses to adopt 'No-BMP'. Thus, for $y_j = x_k$, all Hydrological Response Units (HRUs) [29] in the watershed that grow crop j adopt the same BMP x_k. (\$/km^2) multiplied by the total area of farmers' land that adopt the BMP, to be maximized. Here, we assume that the labor cost is a proxy of the net revenue. Hence, the expected net revenue for a BMP is computed as a fixed fraction (i.e., the labor cost proportion) of its total implementation cost [30]. On the other hand, f_o, also to be maximized, is derived from a categorical variable, where each of the 10 BMPs is categorized into one of five categories based on the expected impact on long-term farm agricultural yield, from 'Significant Decrease' to 'Significant Increase'.

The optimization itself is performed through an exhaustive search. First, all possible BMP combinations are enumerated, which yields $\binom{11}{5} = 462$ (10 possible BMPs + No-BMPs and five land uses) possible BMPs that the UL could theoretically choose from. Then, for each of these enumerated BMP announcements containing five elements, the number of possible farmer adoption scenarios is $5^6 = 15,625$. This is because each of the six LL-DMs can choose any one of the five BMP options. Note that in one scenario (y_i = No-BMP), none of the six LL-DMs chooses a prescribed BMP. Thus, for a given UL policy ($\mathbf{x}$) and each ($\mathbf{y}$) of the farmers' 15,625 options, we can obtain two LL objectives: f_r, and f_o. Then, the dominated LL solutions are removed, and the remaining non-dominated LL solutions are recorded. Subsequently, these non-dominated LL solutions are evaluated for the two UL criteria: F_c and F_s. The procedure is repeated for each of the 462 UL $\mathbf{x}$ solutions. After this extensive and repeated evaluation of the SWAT on all UL solutions, we perform the MED analysis. For our purpose of illustrating the MED concept and its usefulness, considering small UL and LL problems and taking their complete enumeration as a substitute for an optimization algorithm does not trivialize the present study.

C. Results

The computation of UL and LL objective values for non-dominated solutions results in a large and dispersed set of s_p^{opt} in the UL decision space, as shown in Fig. 9. Seven sets of BMP announcement options are found to lie on the optimistic front (Table I). Each optimistic solution is marked with a different maker in the figure. It is interesting that although each UL optimistic solution has exactly five different BMP announcement options in its description, the LL solutions use a maximum of three BMPs to produce their best LL-objective combinations. Taking into consideration all the LL Pareto-optimal solutions of all the optimistic UL solutions, only four of the 10 available BMPs ('tree and shrub establishment', 'upland wildlife habitat management', 'water wells', and 'vegetative barrier') are found to be present in optimistic solutions. This is important byproduct knowledge of the MED task, as it suggests that the remaining six BMPs should have a non-beneficial cost-sediment trade-off in order to be considered as an option to any of the optimistic solutions of the problem.

To find the MED optimistic solution, we normalize F_c and F_s and compute $\Delta(\mathbf{x}_p^*)$ for each optimistic solution

TABLE I
SEVEN DISTINCT UL OPTIMISTIC SOLUTIONS AND THEIR RESPECTIVE LL OPTIONS (WITH MINIMUM COST) ARE SHOWN. 'NO BMP' OPTIONS ARE NOT NOTED IN THE FIRST COLUMN. THE RECOMMENDED MED SOLUTION IS SHOWN IN BOLD.

UL decision variables (BMPs announced)*	LL decision variables (adoption of BMPs)†*						UL objectives		LL objectives		Exp. Dev.
	AF	CN	FP	SG	SY	WT	Cost per BMP (M$)	Sediment (tons/day)	Revenue per BMP (k$)	Change in output (Categorical)	Δ
TSE	No BMP	No BMP	TSE	No BMP	No BMP	No BMP	0.01	3.70	3.36	-416.96	1.23
TSE, UWHM	No BMP	No BMP	TSE	UWHM	No BMP	No BMP	0.03	3.70	4.95	-904.38	1.23
WW, TSE	WW	TSE	WW	WW	TSE	WW	2.86	2.36	692.79	-212250.56	1.11
WW, TSE, UWHM	WW	TSE	UWHM	WW	TSE	WW	2.86	2.36	693.21	-212876.00	1.10
UWHM	No BMP	No BMP	UWHM	No BMP	No BMP	No BMP	0.01	3.70	0.68	-208.48	1.16
TSE, VB	**VB**	**TSE**	**VB**	**TSE**	**TSE**	**TSE**	**3.13**	**2.34**	**759.33**	**-268482.25**	**0.02**
TSE, WW, VB	VB	TSE	WW	TSE	TSE	WW	2.94	2.36	704.28	-232439.51	1.14

*TSE: 'Tree & shrub establishment'; UWHM: 'Upland wildlife habitat management'; WW: 'Water well'; VB: 'Vegetative barrier'
†AF: Alfalfa; CN: Corn; FP: Field peas; SG: Sugar beets, SY: Soy beans, WT: Winter wheat

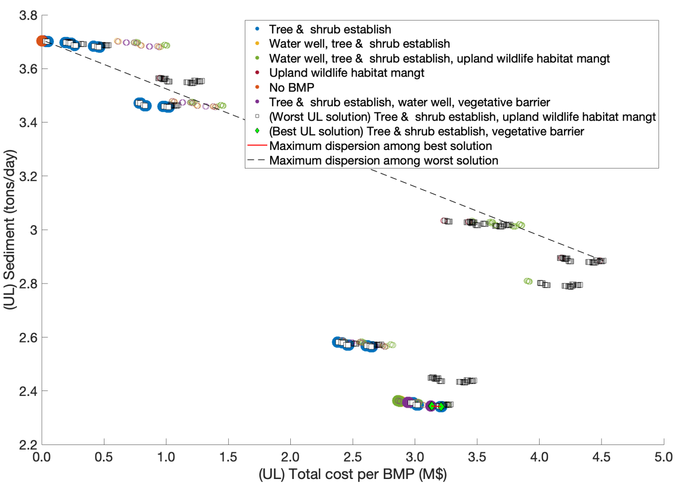

Fig. 9. UL solutions of the agricultural management problem, in which both objectives are minimized. Each colored circle corresponds to a different member of s_p^{opt}, and the best (spanning only from 3.13 to 3.21 M$ cost) and worst (spanning widely from 0.03 to 4.52 M$ cost) options in terms of expected deviation arising from LL solutions are marked with green diamonds and white squares, respectively. Dominated solutions are shown with transparent centers.

$\mathbf{x}_p^*$. The UL-DMs then choose the member of $\mathbf{x}_p^*$ with the minimum $\Delta(\mathbf{x}_p^*)$. The optimistic front, $(\mathbf{x}_p^*)$, which is disjointed, spans from 2.35 to 3.8 tons/day for F_s, and from zero to \$3.5M for F_c (Fig. 9). The pseudo-pessimistic front is skewed from the optimistic front, ranging between 2.8 to 3.6 sediment tons/day for F_s, and between \$500K and \$5M for F_c. We ignore the trivial all 'No-BMP' solution from our decision-making analysis, as our goal is to increase farmers' adoption of BMPs. Interestingly, six UL solutions recommend the use of a specific BMP – 'tree & shrub establishment', making it the single-most important BMP among all BMPs considered here. For the remaining seven optimistic UL solutions, the normalized $\Delta(\mathbf{x}_p^*)$ values range from 0.02 to 1.23 (Table I). The lowest $\Delta(\mathbf{x}_p^*)$ solution (our MED solution with $\Delta = 0.02$) has the BMP pair 'tree & shrub establishment' and 'vegetative barrier', which is marked with green diamonds in Figs. 9 and 10. The first figure shows that the difference in the three green diamonds is the least, compared to the other colors. This is why this solution corresponds to the preferred solution of the UL-DM, since it minimizes

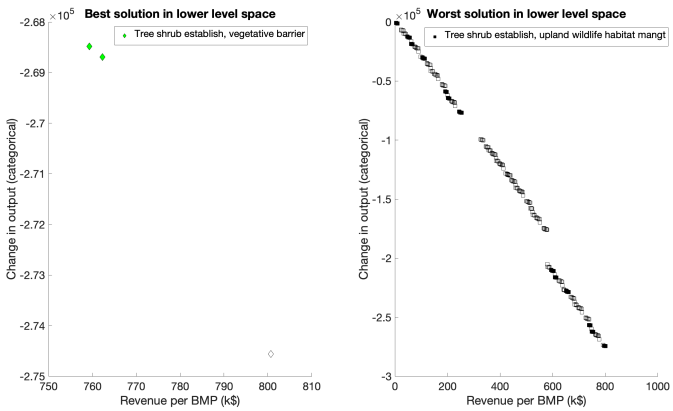

Fig. 10. LL Pareto-optimal choices for the best (left) and worst (right) UL MED choices. Note that although many of these solutions are dominated in the UL space (Fig. 9), they are all non-dominated in the lower-level space, since they are the best solutions from the farmers' (LL-DM) perspective. Solutions that are dominated in the upper-level have transparent centers.

the risk by causing relatively little deviation arising from the LL-DM decision. The worst deviation comes from the BMP pair 'tree & shrub establishment' and 'upland wildlife habitat management' having $\Delta = 1.23$, causing this solution to result in an outcome that is 61.5 times more deviated in the cost-sediment values compared to the preferred solution ('tree & shrub establishment' and 'vegetative barrier'). This case study illustrates how our proposed MED approach can help UL-DMs choose a better predicted solution by first finding Pareto optimistic solutions and then selecting one that causes the minimum expected deviation in their objectives due to the independence of LL-DMs. Fig. 10 shows the respective LL Pareto front for the MED optimistic solution (left figure) and the worst-deviation optimistic solution (right figure). The trade-off between the two LL objectives is clearly visible in both figures. Importantly, the worst-deviation solution is associated with many LL Pareto solutions, thereby providing farmers with more options to choose from. Although this may be excellent from the farmer's point of view, it causes a large dispersion in the UL objective values. Since the UL-DMs have greater control over the final choice of solution, choosing a MED solution with only three LL options causes the minimum deviation in cost-sediment trade-off at the upper level.

VI. Telecommunication Management Problem

A cellular network contains a number of different elements ranging from the Base Transceiver Station (BTS) with its antenna to a Base Station Controller (BSC). A BTS performs direct communications with mobile phones. Typically, small numbers of base stations are linked to a BSC, which is responsible for routing calls to the required base station. Fig. 11 shows a sketch of a cellular network structure [31]. The location of a BTS is an important factor in achieving a high cell planning efficiency. It can be dealt with as an optimization problem with a few network planning parameters, such as the traffic density, channel condition, interference scenario and number of base stations. The problem, by its very nature, is a multi-objective problem, as it requires maximizing coverage, minimizing the radiation effect, minimizing cost by minimizing the number of BTSs, and other criteria [32]. Clearly, the telecommunication management problem has two hierarchical levels of tasks and decision-makers: (i) locating the BTSs in a service area, leading to a trade-off between minimizing the installation cost and the radiation effect managed by the telecommunication companies, and (ii) adjusting the strength and orientation of coverage by each BTS unit locally so that there is uniformity in the traffic flow among BTSs to allow smooth service and the minimum coverage inefficiency (sum of under- and overcoverage) to be managed by each BTS service provider.

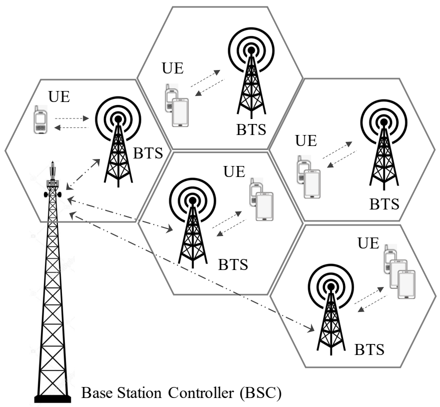

Fig. 11. Overview of the telecommunication management problem. "BTS" refers to the base transceiver station, and "UE" refers to user equipment.

A. Problem Description

A given service area (A) with exact locations (in (ξ,η) coordinates) of W customers is chosen. From a higher-level management perspective for infrastructure planning, the UL problem must determine the number of BTSs (B) and their locations (in ξ-η coordinates). The variables of the UL are $\mathbf{x} = [B, \{(\xi_i, \eta_i), i = 1, \ldots, B\}]$ with $x_1 = B$. This means that the UL variable vector ($\mathbf{x}$) is of varying length. The LL variable vector ($\mathbf{y}$) is described below. The UL problem involves two objectives to be minimized: infrastructure investment ($F_1(\mathbf{x},\mathbf{y}) = \Pi(\mathbf{x},\mathbf{y})$) and average radiation in terms of the transmitted power of all BTSs ($F_2(\mathbf{x},\mathbf{y}) = R(\mathbf{x},\mathbf{y})$):

$$\Pi(\mathbf{x},\mathbf{y}) = n_{\text{conn}}(\mathbf{x},\mathbf{y})\omega_{\text{conn}} + x_1\omega_{\text{bts}}, \tag{15}$$

$$R(\mathbf{x},\mathbf{y}) = \frac{1}{x_1}\sum_{i=1}^{x_1} 4\pi P_d y_{2i-1}^2 10^{-0.1G}, \tag{16}$$

where $n_{\text{conn}}(\mathbf{x},\mathbf{y})$ is the number of connections that need to be made by all BTSs depending on their strength and orientation set in the LL and the allowed number of customers per connection (τ). The problem parameter values used in this study are presented in Table II. B varies within [5, 10]. To avoid using a variable-length algorithm, we run our BLEMO method independently for each B and then combine the results for MED analysis.

TABLE II
Parameters of the Telecommunication management problem.

Parameter	Description	Value (unit)
ω_{bts}	BTS cost	300 ($ k)
ω_{conn}	connection cost	100 ($ k)
P_d	power density	22.5 (watts/m^2)
G	gain of antenna	12 (dB)
τ	connection threshold	1,000 (/conn.)

Given the number and fixed location of BTSs at the UL, the LL problem attempts to find the strength of coverage (S_i) and the orientation (θ_i) from the x-axis (east direction) of each BTS (direction of maximum transmission) to minimize two objectives: the standard deviation of the traffic flow to each BTS ($f_1(\mathbf{x},\mathbf{y}) = \sigma(\mathbf{x},\mathbf{y})$) and the coverage inefficiency (sum of undercovered and overcovered regions) of the service area ($f_2(\mathbf{x},\mathbf{y}) = \rho(\mathbf{x},\mathbf{y})$). The LL variables are $\mathbf{y} = (\{(S_i,\theta_i), i = 1,\ldots,B\})$. The coverage area for each BTS is considered to vary in a hexagonal form around the BTS – a common practice used in the telecommunication literature. The orientations of the hexagons and their sizes are controlled by the LL variables. Two constraints are included to obtain meaningful solutions: (i) g_1: the total fraction of undercovered customers must be less than 5% of the total number of customers and (ii) g_2: the total overcovered customers must be less than 10% of the total number of customers.

The undercovered and overcovered customers are determined as follows: For the given distribution of W customers in a region (shown with a dot in the figures in the results section), the coverage by a BTS is determined from the LL variable vector (strength and orientation of transmission). The fraction of customers covered by the i-th BTS ($c_i(\mathbf{x},\mathbf{y})$) is first calculated from the total number of customers ($C_i(\mathbf{x},\mathbf{y})$) at the BTS divided by W, and then the standard deviation of c_i is defined as the first LL objective. The proportion of all customers who are outside the coverage area of all BTSs is termed the undercovered fraction ($u(\mathbf{x},\mathbf{y})$). Likewise, the proportion of customers who are covered by more than one BTS is termed the overcovered fraction ($o(\mathbf{x},\mathbf{y})$). Thus, the first LL objective is determined as the standard deviation of the

c_i values. The second LL objective, coverage inefficiency, is defined as $\rho(\mathbf{x}, \mathbf{y}) = u(\mathbf{x}, \mathbf{y}) + o(\mathbf{x}, \mathbf{y})$. The LL problem also calculates the number of connections (n_{conn}) needed to cover the customers, which is needed for computing the UL objective Π. For a connection limit of τ customers, n_{conn} is computed as follows: $n_{\text{conn}}(\mathbf{x}, \mathbf{y}) = \sum_{i=1}^{x_1} \left\lceil \frac{C_i(\mathbf{x},\mathbf{y})}{\tau} \right\rceil$. Operator $\lceil \cdot \rceil$ makes the above function non-differentiable. Additionally, the LL objectives are difficult to express in a mathematical function, so any derivative can be computed for the purpose of carrying out a gradient-based optimization algorithm. The bi-level, bi-objective telecommunication problem is formulated as follows:

$$\begin{aligned} \text{Minimize} \quad & {}_{\mathbf{x} \in \mathbf{X}, \mathbf{y} \in \mathbf{Y}} F(\mathbf{x}, \mathbf{y}) = (\Pi(\mathbf{x}, \mathbf{y}), R(\mathbf{x}, \mathbf{y})), \\ \text{subject to} \quad & \mathbf{y} \in \underset{\mathbf{y} \in \mathbf{Y}}{\text{argmin}} \{ f(\mathbf{x}, \mathbf{y}) = (\sigma(\mathbf{x}, \mathbf{y}), \rho(\mathbf{x}, \mathbf{y})) | \\ & g_1(\mathbf{x}, \mathbf{y}) \leq 0, g_2(\mathbf{x}, \mathbf{y}) \leq 0 \}, \end{aligned} \tag{17}$$

where $\mathbf{x} = (B, \{(\xi_i, \eta_i), i = 1, \ldots, B\})$ and $\mathbf{y} = (\{(S_i, \theta_i), i = 1, \ldots, B\})$. Note that $B = x_1$ is a positive integer.

B. Computational Procedure

To handle the mixed nature of UL variables (integer and continuous), we implement a computationally fast method for this study. For a specific B, we use the k-means clustering method on the W customer locations to find a good position (ξ_i, η_i) for each of the B BTSs. The BLEMO algorithm [12] is used to find optimistic UL solutions. Then, for each UL solution, an LL optimization is performed to find $M_p = 100$ Pareto-optimal LL solutions to determine the final MED solution ($\mathbf{s}^{\text{pref}}$). For the UL, we use a population size of 100 and run the algorithm for a maximum of 2,000 generations. For each LL, we use a population size of 100 and run it for 1,000 generations. While these numbers were arrived at after some trial and error simulations, the purpose of this paper is not to develop the most efficient BLEMO algorithm but rather to present the working and importance of the proposed MED methodology. The other NSGA-II parameters are kept at their standard values [22].

C. Results

Fig. 12 shows the optimistic Pareto solutions in the UL objective space with open circles. Notably, all six B-values are present in the front, and for some BTSs, there is more than one ($Q_p > 1$) optimistic solution. It is clear that with more investment in BTS installations, the radiation level can be reduced. For each B, the respective location of each BTS and its strength can be obtained from the optimistic solutions. For $B = 6$, the respective LL Pareto-optimal front is shown in Fig. 13. The coverage level of each BTS is marked with a hexagon, and the size of the hexagon signifies its strength. Notice that the locations of each hexagon (UL vector) is identical in all three LL solutions, but their sizes and orientations are different for different LL solutions. The worst (pessimistic) points obtained by the D-MED approach are shown in Fig. 12 with open squares. The MED analysis reveals that $B = 9$ produces the minimum deviation due to the independence of LL decision-making. However, if a maximum investment limit of 2M\$ is fixed for the study, then only $B = 5$ and 6 are allowed, and the MED solution will correspond to $B = 5$.

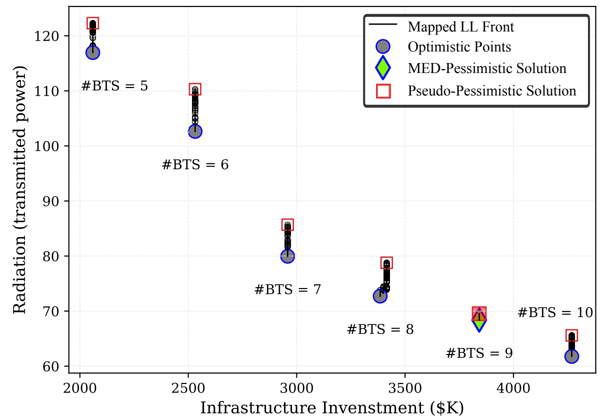

Fig. 12. Optimistic solutions in the UL objective space for the telecommunication management problem. The $B = 9$ solution has the minimum MED and is the preferred solution.

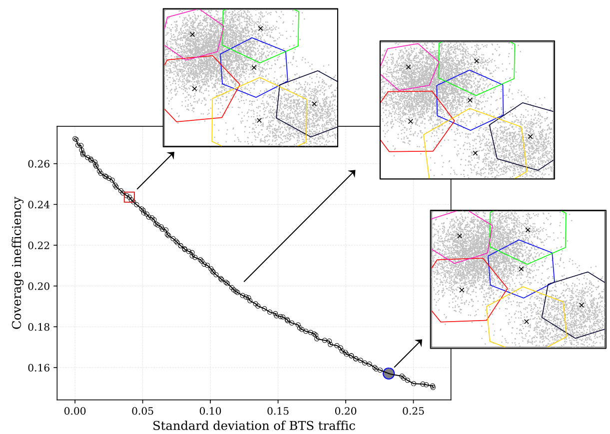

Fig. 13. Three LL Pareto-optimal solutions for the $B = 6$ BTS case. The locations of the six BTSs are fixed in all solutions, but the coverage strengths (sizes of the hexagons) and orientations are different, causing a trade-off in the LL problem.

Table III presents the six optimistic solutions and their respective UL and LL objective values. The MED solution ($B = 9$, shown in Fig. 12) corresponds to the LL variable $\theta^* = 0.0190$ rad and causes a 76.9% reduced deviation in the expected outcome compared to another optimistic solution chosen at random ($\theta_{avg} = 0.0822$ rad). The MED solution also causes approximately an 85% reduced deviation from the worst deviated optimistic solution with $B = 6$ having $\theta_{max} = 0.1267$ rad. The optimal preferred configuration with $B = 9$ is shown in Fig. 14.

This case study shows how the ideas proposed in this paper can be used for analysis by a telecommunication provider to develop an optimal number of BTSs that will allow them to have a minimum deviation from their investment-radiation targets, which may have been caused

TABLE III
THE RELEVANT PROPERTIES OF THE SIX OPTIMISTIC SOLUTIONS OBTAINED BY THE BL-EMO PROCEDURE ARE SHOWN. ONLY #BTS OF THE UL VARIABLES IS SHOWN, BUT BOTH LL VARIABLES (STRENGTH AND ORIENTATION) ARE PRESENTED. THE 9-BTS SOLUTION HAS THE MINIMUM EXPECTED DEVIATION.

#BTS	Strength	Orientation	UL objectives		LL objectives		Exp. Dev.
	S (unit)	θ (rad)	Π ($)	R	σ	ρ	δ
5	[2.495, 3.081, 2.696, 2.599, 1.931]	[0.443, -0.824, 0.599, 0.186, 0.225]	2.059e+3	1.169e+2	9.715e-3	1.957e-1	0.0884
6	[2.143, 2.643, 2.527, 2.467, 2.041, 2.569]	[-0.459, 0.046, 0.511, 0.377, 0.380, -0.420]	2.531e+6	1.026e+2	2.318e-1	1.571e-1	0.1267
7	[2.681, 1.454, 1.948, 1.993, 2.136, 2.161, 2.445]	[0.115, 0.228, 0.111, -0.520, 0.125, 0.410, -0.224]	2.958e+6	7.995e+1	4.862e-1	1.819e-1	0.0949
8	[2.065, 1.583, 2.177, 1.715, 2.012, 2.144, 2.279, 2.178]	[-0.102, 0.185, 0.225, 0.349, -0.007, 0.236, 0.313, 0.304]	3.385e+6	7.272e+1	4.151e-1	1.506e-1	0.1010
9	**[2.039, 1.463, 2.124, 2.410, 1.655, 2.365, 2.711, 1.852, 1.002]**	**[0.214, -0.221, 0.490, 0.209, -0.205, 0.275, 0.253, 0.057, -0.057]**	**3.842e+6**	**6.838e+1**	**7.261e-3**	**1.955e-1**	**0.0190**
10	[1.729, 1.296, 1.431, 2.305, 1.705, 2.510, 2.553, 1.717, 1.000, 2.363]	[-0.400, -0.044, -0.323, 0.276, 0.053, 0.177, 0.274, -0.175, -0.394, 0.371]	4.269e+6	6.177e+1	4.249e-2	1.514e-1	0.0631

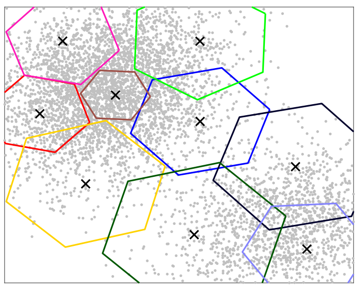

Fig. 14. The preferred MED solution with 9 BTSs at the lower-level is shown for the telecommunication problem. While the number of BTSs and their locations are determined by the UL, each BTS's strength and orientation are determined by the LL.

by the independent decisions of the service providers during operation. A random choice of another optimistic BTS arrangement would cause 94.5% more deviation from their expected investment-radiation targets. Notably, if the telecommunication provider prefers a smaller maximum investment budget of $3M, a 5-BTS solution (with $\delta = 0.0884$) would be the preferred MED solution.

VII. CONCLUSIONS

In hierarchical systems involving two or more decision-making groups (DMs), while the upper level DMs (usually policy makers) have more control, lower- and intermediate-level independent decision-making tasks often prevent them from achieving their desired overall goals involving investment cost and environmental effects. This paper has proposed a novel decision-making concept: choosing an upper-level solution that would minimize the deviation in the expected goals due to the independent nature of decision-making at the lower-level. Four different approaches have been proposed. After presenting the basic concept through a bi-level, multi-objective programming problem, proof-of-principle results are presented on two test problems. Then, the concept has been applied to two societal management problems – agricultural and telecommunication networking problems – to demonstrate the usefulness of the proposed approach.

This concept can be extended to multi-level problems having more than two levels and problems having more than two objectives at each level. Since the final outcome is a single solution corresponding to the minimum expected deviation, finding novel ways of solving the direct problem (Equation 10) in a single simulation would be an interesting but a challenging optimization task. If the preference information of the UL objectives is known a priori, Equation 4 can be modified according to various MCDM techniques. By knowing the probabilistic preference structure of LL-DMs, the δ calculation can be converted to an expected δ metric by using the probability structure of LL-DMs. Nevertheless, we believe that the proposed MED concept is pragmatic for hierarchical problems and is now ready to be extended and applied to various other real-world application problems.

ACKNOWLEDGEMENT

This material is based in part upon work supported by the National Science Foundation under Cooperative Agreement No. DBI-0939454. Any opinions, findings, and conclusions or recommendations expressed in this material are those of the author(s) and do not necessarily reflect the views of the National Science Foundation.

REFERENCES

[1] J. F. Bard, Practical bilevel optimization: algorithms and applications. Springer Science & Business Media, 2013, vol. 30.
[2] A. Sinha, P. Malo, and K. Deb, "A review on bilevel optimization: from classical to evolutionary approaches and applications," IEEE Transactions on Evolutionary Computation, vol. 22, no. 2, pp. 276–295, 2017.
[3] Y. Wang, Y. C. Jiao, and H. Li, "An evolutionary algorithm for solving nonlinear bilevel programming based on a new constraint-handling scheme," IEEE Transactions on Systems, Man, and Cybernetics, Part C: Applications and Reviews, vol. 32, no. 2, pp. 221–232, 2005.
[4] D. Hadka and P. Reed, "Large-scale parallelization of the borg multiobjective evolutionary algorithm to enhance the management of complex environmental systems," Environmental Modelling & Software, vol. 69, pp. 353–369, 2015.
[5] K. Li, Z. Xiang, T. Chen, and K. C. Tan, "BiLO-CPDP: Bi-level programming for automated model discovery in cross-project defect prediction," in 2020 35th IEEE/ACM Intl. Conf. on Automated Software Engineering (ASE), 2020, pp. 573–584.
[6] A. Sinha, P. Malo, K. Deb, P. Korhonen, and J. Wallenius, "Solving bilevel multicriterion optimization problems with lower level decision uncertainty," IEEE Transactions on Evolutionary Computation, vol. 20, no. 2, pp. 199–217, 2016.
[7] D. Colander and R. Kupers, "Complexity and the art of public policy: Solving society's problems from the bottom up," 2014.
[8] F. A. Hayek, "The use of knowledge in society," The American economic review, vol. 35, no. 4, pp. 519–530, 1945.
[9] B. Mueller, "Why public policies fail: Policymaking under complexity," EconomiA, vol. 21, no. 2, pp. 311–323, 2020.
[10] F. Squazzoni, "A social science-inspired complexity policy: Beyond the mantra of incentivization," Complexity, vol. 19, no. 6, pp. 5–13, 2014.
[11] S. Dempe, Foundations of bilevel programming. Secaucus, NJ, USA: Kluwer Academic Publishers, 2002.

[12] K. Deb and A. Sinha, "An efficient and accurate solution methodology for bilevel multi-objective programming problems using a hybrid evolutionary-local-search algorithm," Evolutionary Compuation Journal, vol. 18, no. 3, pp. 403–449, 2010.
[13] M. M. Islam, H. K. Singh, T. Ray, and A. Sinha, "An enhanced memetic algorithm for single-objective bilevel optimization problems," Evol. Comput. Journal, vol. 25, no. 4, pp. 607–642, 2017.
[14] L. Chen, H.-L. Liu, K. C. Tan, and K. Li, "Transfer learning based parallel evolutionary algorithm framework for bi-level optimization," IEEE Transactions on Evolutionary Computation, pp. 1–1, 2021.
[15] N. Gupta, M. Khosravy, N. Patel, and T. Senjyu, "A bilevel evolutionary optimization for coordinated transmission expansion planning," IEEE Access, vol. 6, pp. 48 455–48 477, 2018.
[16] G. Whittaker, R. Färe, S. Grosskopf, B. Barnhart, M. Bostian, G. Mueller-Warrant, and S. Griffith, "Spatial targeting of agri-environmental policy using bilevel evolutionary optimization," Omega, vol. 66, pp. 15–27, 2017.
[17] Z. Guo, D. Zhang, S. Y.-S. Leung, and L. Shi, "A bi-level evolutionary optimization approach for integrated production and transportation scheduling," Applied Soft Computing, vol. 42, pp. 215–228, 2016.
[18] A. Gupta, J. Mańdziuk, and Y.-S. Ong, "Evolutionary multitasking in bi-level optimization," Complex & Intelligent Systems, vol. 1, no. 1-4, pp. 83–95, 2015.
[19] K. Deb, J. Sundar, N. Uday, and S. Chaudhuri, "Reference point based multi-objective optimization using evolutionary algorithms," International Journal of Computational Intelligence Research (IJCIR), vol. 2, no. 6, pp. 273–286, 2006.
[20] K. Miettinen, Nonlinear Multiobjective Optimization. Boston: Kluwer, 1999.
[21] K. Deb, Multi-objective optimization using evolutionary algorithms. Chichester, UK: Wiley, 2001.
[22] K. Deb, S. Agrawal, A. Pratap, and T. Meyarivan, "A fast and elitist multi-objective genetic algorithm: NSGA-II," IEEE Tran. on Evol. Comput., vol. 6, no. 2, pp. 182–197, 2002.
[23] J. Mateo-Sagasta, S. M. Zadeh, and H. Turral, More people, more food, worse water?-A global review of water pollution from agriculture. Rome: Food and Agriculture Organization of the UN and Int. Water Management Inst., 2018.
[24] R. Lal, "Soil erosion impact on agronomic productivity and environment quality," Critical reviews in plant sciences, vol. 17, no. 4, pp. 319–464, 1998.
[25] M. R. McCorve and C. L. Lant, "Drainage district formation and the loss of midwestern wetlands, 1850-1930," Agricultural History, vol. 67, no. 4, p. 13, Fall 1993.
[26] C. Smith, J. Williams, A. P. Nejadhashemi, S. Woznicki, and J. Leatherman, "Cropland management versus dredging: An economic analysis of reservoir sediment management," Lake and reservoir management, vol. 29, no. 3, pp. 151–164, 2013.
[27] R. Eeswaran, A. P. Nejadhashemi, and S. R. Miller, "Evaluating the climate resilience in terms of profitability and risk for a long-term corn-soybean-wheat rotation under different treatment systems," Climate Risk Management, vol. 32, p. 100284, 2021.
[28] J. G. Arnold, D. N. Moriasi, P. W. Gassman, K. C. Abbaspour, M. J. White, R. Srinivasan, C. Santhi, R. Harmel, A. Van Griensven, M. W. Van Liew et al., "SWAT: Model use, calibration, and validation," Transactions of the ASABE, vol. 55, no. 4, pp. 1491–1508, 2012.
[29] M. M. Kalcic, I. Chaubey, and J. Frankenberger, "Defining soil and water assessment tool (SWAT) hydrologic response units by field boundaries," International Journal of Agricultural and Biological Engineering, vol. 8, no. 3, pp. 69–80, 2015.
[30] NRCS, "Michigan payment schedules," 2020. [Online]. Available: https://www.nrcs.usda.gov/wps/portal/nrcs/detail/national/programs/financial/?cid=nrcseprd1328244
[31] M. Job, K. Anish, and V. W. Ben, "Optimization of antenna placement in 3G networks using genetic algorithms," in Proceedings of IEEE Third International Conference on Broadband communication, Information Technology and Biomedical Applications, 2008, pp. 30—37.
[32] K. Lieska, E. Laitinen, and J. Lahteenmaki, "Radio coverage optimization with genetic algorithms," in Ninth IEEE International Symposium on Personal, Indoor and Mobile Radio Communications, vol. 1. IEEE, 1998, pp. 318–322.

Kalyanmoy Deb is University Distinguished Professor and Koenig Endowed Chair Professor at the Department of Electrical and Computer Engineering at Michigan State University (MSU), East Lansing, USA. Prof. Deb's research interests are in evolutionary optimization algorithms and application in optimization and machine learning. He is a fellow of IEEE and ASME. He has written more than 580 research papers and received many awards including Infosys prize and Edgeworth Pareto award.

Zhichao Lu received his Ph.D. degree in Electrical and Computer Engineering from Michigan State University, USA, in 2020. He is currently a post-doc research fellow at Southern University of Science and Technology, China. His research interests include machine learning assisted evolutionary algorithms, automated machine learning, and in particular evolutionary neural architecture search. He received the GECCO-2019 best paper award.

Ian Kropp is a Ph.D. student in Biosystems & Agricultural Engineering and Computer Science Engineering at Michigan State University. He designs algorithms that develop sustainable agricultural management practices, while simultaneously balancing environmental, social, and economic goals. His primary research interest is in merging mathematical optimization and human decision making through multi-objective optimization.

J. Sebastian Hernandez-Suarez is a postdoctoral scholar at Stanford University, where he applies artificial intelligence and numerical modeling for understanding complex water resources systems and supporting environmental decision-making. He received his Ph.D. degree in Biosystems Engineering from Michigan State University in 2021.

Rayan Hussein received B.Sc. and M.Sc. degrees in electrical and communication engineering from the University of Mosul, Mosul, Iraq, in 2002 and 2005, respectively. He was with an industrial mobile telecom company, Iraq, from 2005 to 2013. His current research interests include evolutionary computation with a focus in metamodeling for constrained multiobjective optimization problems.

Steven Miller received his Ph.D. degree in Economics from Oklahoma State University, USA, in 2005. He is currently the Director of the MSU Center for Economic Analysis, where his research focus includes developing methods and models for measuring economic impact for policy and industry simulation.

A. Pouyan Nejadhashemi received his Ph.D. in biological resources engineering from the University of Maryland in 2006. He is currently Michigan State University Foundation Professor in the Department of Biosystems and Agricultural Engineering and the Department of Plant, Soil and Microbial Sciences. As a leading expert in environmental modeling, he examines water and its distribution, movement and quality in a variety of environments.